PHILOSOPHICAL TRANSACTIONS OF THE ROYAL SOCIETY A MATHEMATICAL, PHYSICAL & ENGINEERING SCIENCES

The Surface Structure and Composition of Layered Silicate Minerals: Novel Insights from X-Ray Photoelectron Diffraction, K-Emission Spectroscopy and Cognate Techniques

S. Evans, J. M. Adams and J. M. Thomas

Phil. Trans. R. Soc. Lond. A 1979 **292**, 563-591
doi: 10.1098/rsta.1979.0074

THE SURFACE STRUCTURE AND COMPOSITION OF LAYERED SILICATE MINERALS: NOVEL INSIGHTS FROM X-RAY PHOTOELECTRON DIFFRACTION, K-EMISSION SPECTROSCOPY AND COGNATE TECHNIQUES

By S. Evans,† J. M. Adams† and J. M. Thomas, F.R.S.‡

† *Edward Davies Chemical Laboratories, University College of Wales, Aberystwyth, Dyfed, SY23 1NE, U.K.*

‡ *Department of Physical Chemistry, Lensfield Road, Cambridge, CB2 1EP, U.K.*

(*Received* 27 *November* 1978 – *Revised* 14 *March* 1979)

CONTENTS

Angle-resolved X-ray photoelectron spectra of freshly exposed cleavage planes of muscovite, lepidolite, phlogopite, and both natural and Pb-exchanged vermiculite are interpreted to yield both quantitative elemental analyses relating to the outermost 100 Å of the crystals and a wealth of structural information, the latter from

consideration of phenomena resulting from diffraction of the photo-emitted electrons. It is demonstrated that X-ray photoelectron diffraction can be used to differentiate between equivalent, near-equivalent, and non-equivalent sites occupied by two (or more) elements either in one single crystal or in crystals of closely similar structure, even when the element(s) concerned comprise only a small fraction of the crystal and when the sub-lattice lacks both long- and short-range order.

These studies are complemented by extensive chemical analyses, by energy-dispersive X-ray (K-emission) analyses performed in an electron microscope (an elementary calibration procedure for which is outlined) and by X-ray diffraction studies. The muscovite and lepidolite are shown to cleave in regions exhibiting typical bulk composition, whereas the phlogopite and vermiculite both cleave in regions rich in aluminium, and deficient in magnesium (relative to their silicon content). The principal interlayer cations in the vermiculite, potassium and calcium, could be entirely replaced with lead by prolonged refluxing in lead nitrate solution: the lead and calcium are shown to retain their hydration spheres whereas potassium coordinates directly (without hydration) to the layer oxygen, as in the true micas.

Some structural implications of these data are evaluated and discussed.

1. Introduction

An important objective of our activities in electron spectroscopy in recent years has been to establish procedures by which quantitative surface analytical information might be reliably obtained from X-ray photoelectron spectroscopy (X.p.s.). In the first of three recent reports on this objective (Adams *et al.* 1977; Evans *et al.* 1977, 1978), we demonstrated (by comparison of chemical and X.p.s. analyses) that X.p.s. could yield quantitative data accurate to *ca.* 5% for homogeneous polycrystalline solids, as exemplified by a series of naturally occurring aluminosilicates. During the progress of that work, however, we found one mineral (a highly crystalline phlogopite of Norwegian origin) in which every cleavage plane examined yielded X.p.s. analyses radically different from the independently established bulk composition. Although the existence of such phenomena had not been entirely unsuspected on general grounds relating to chemical microheterogeneity and preferential stratification, no direct evidence for their occurrence had previously been forthcoming. In the present work, we investigate the phenomenon in detail, employing more extensive chemical analyses than in the earlier work and an X.p.s. study in which the variations of the spectra with electron take-off angle are comprehensively explored. These experiments are complemented by energy-dispersive X-ray (K-emission) analyses, carried out in a high-resolution transmission electron microscope, and by X-ray crystallography. Similar measurements have also been undertaken for other related minerals (principally muscovite, lepidolite, and vermiculite – both natural and ion-exchanged), and taken as a whole these data allow us to describe the structural chemistry appropriate to the regions in which these rather complex solids cleave with far more certainty than would have been possible before the advent of modern surface-sensitive techniques such as X.p.s.

This work is not, however, solely of geochemical significance: in our interpretation of the angle-resolved X.p.s. we have, in effect, identified a new and widely applicable way of deriving directly structural information relevant to the outermost 100 Å† or less of a single-crystal specimen from a technique hitherto regarded as useful only in electronic and analytical contexts, as explained briefly in two preliminary communications (Adams *et al.* 1978*a*, *b*). This new information, moreover, is frequently of a kind which cannot be obtained as easily – if

† 1 Å = 0.1 nm = 10^{-10} m.

PHILOSOPHICAL TRANSACTIONS OF THE ROYAL SOCIETY A MATHEMATICAL, PHYSICAL & ENGINEERING SCIENCES

at all – from established methods for the determination of structure in the solid state. The spectroscopic data are most conveniently displayed in a form quite different from the usual X.p.s. presentation, and to make the distinction clear we shall refer to the relevant diagrams as 'X-ray photoelectron diffraction (X.p.d.) patterns', the new structural information being derived by virtue of the diffraction of the outgoing photoelectrons by the atoms surrounding the emitting site.

Although the existence of these diffraction phenomena has been known for some years (Siegbahn *et al.* 1970; Fadley & Bergström 1971), their potential value in structural chemical studies of the near-surface regions of single-crystal solids does not previously appear to have been recognised, despite the early observation by Fadley & Bergström (1971) that the angular dependence of the X.p.s. signal from silver dissolved in single-crystal gold was essentially identical with that relating to the majority component. The apparently low level of interest in the phenomenon may have arisen from the difficulties inherent in accounting quantitatively for the individual diffraction patterns: at these relatively low electron energies multiple scattering effects cannot be neglected, and the problem is reminiscent of the difficulties encountered in the quantitative interpretation of low energy electron diffraction (l.e.e.d.) intensity data. Although considerable advances have been made for the simpler crystals, a semi-quantitative theoretical reproduction of the diffraction patterns from a single crystal of gold having recently been achieved (Baird *et al.* 1977), the *ab initio* prediction of X.p.d. patterns for materials as complex in structure as the layered silicates still seems some way into the future. The interpretations advanced in this paper are thus necessarily based almost entirely on qualitative considerations. However, the fact that valuable structural data can be obtained without any complex computational work renders X.p.d. particularly attractive as a tool to complement other, well-established, techniques in structural studies of large single crystals. X.p.d. may also prove useful in conjunction with the two recently-developed techniques known as 'extended X-ray absorption fine structure' (e.X.a.f.s.) and 'extended electron energy loss fine structure' (ex. e.l.f.s.) – see Stern (1974), Bassi *et al.* (1976), and Leapman & Cosslett (1976) or Kincaid *et al.* (1978) respectively. These techniques are, however, also capable of yielding information concerning the location of guest atoms in solids completely lacking in long range crystallographic order.

2. Experimental

Large well-crystallized specimens of Norwegian muscovite and phlogopite, and of Brazilian lepidolite, were selected from material supplied by G. Bottley & Co. Vermiculite samples were selected from material originating in the Transvaal, supplied by I.C.I. Ltd. The samples of lead-exchanged vermiculite were prepared from the flakes used for the first X.p.s. study (q.v.) by refluxing them in 0.5 M lead nitrate solution for *ca.* 20 days. After removal from this solution, they were rinsed several times with deionized water and allowed to dry.

The polycrystalline samples of synthetic hectorite ('Laponite') used in calibrating the X-ray analyses in the electron microscope (see below) were supplied by Laporte Industries.

(*a*) *Chemical analyses*

Representative samples (2×0.5 g) of each selected specimen were ground to a fine powder and analysed by using essentially standard literature procedures (Bennett & Reed 1971). The

vermiculite was analysed only in its natural form, before ion-exchange. Initial dissolution occurred, in each case, via fusion with sodium hydroxide: silicon was then determined gravimetrically as quinoline silicomolybdate, aluminium gravimetrically as the 8-hydroxyquinolate, iron colourimetrically as the ferrous *o*-phenanthrolene complex, magnesium and calcium (together) volumetrically by using EDTA with methyl thymol blue complexone indicator, calcium nephelometrically as the oxalate (Adams & Evans 1979), and fluoride by a standard addition technique employing a LaF_3 ion-selective electrode (Thomas *et al.* 1977). All determinations were carried out at least in duplicate. The absence of significant quantities of lithium in all the minerals except lepidolite was confirmed by semi-quantitative atomic emission measurements at 670.8 nm.

(*b*) *Electron spectroscopic measurements*

All measurements were made on the AEI ES 200A instrument used in our previous work on photoionisation cross sections and mineral analysis by X.p.s. (Adams *et al.* 1977; Evans *et al.* 1977, 1978). The preparation chamber of this instrument was equipped with a stainless steel razor blade mounted on a controlled edge-welded bellows assembly (basically a V.G. WS2) to permit the cleavage of appropriately-mounted specimens in ultra-high vacuum (u.h.v.). Monocrystalline mineral flakes were cut to *ca.* 17 mm × 7 mm × 2 mm and were attached to a (truncated) copper probe tip by an 8 BA stainless steel screw. The probe used was rotatable without break of vacuum and had an angular scale permitting changes in angle to be recorded to *ca.* ± 2°; initial alignment was by inspection and the absolute angles are thus less accurately known (*ca.* 10°). In favourable circumstances, up to five cleavages could be obtained from one specimen without break of vacuum, and this system proved successful for all the single-crystal samples except the lead-exchanged vermiculite, which was very difficult to cleave in such a way as to leave a sufficiently large (*ca.* 12 mm × 5 mm) intact flat surface. The two specimens of this that were examined were therefore obtained by cleavage in air and were mounted on a standard probe tip immediately before insertion into the vacuum system, as in our previous studies (Adams *et al.* 1977).

Initially, wide-scan (400–1250 eV) spectra were obtained for each cleavage, followed by detailed scans of all the principal peaks. In most cases, further sets of detail spectra were then recorded as a function of the orientation of the specimen with respect to the incident-photon and detected-electron directions, which in the ES 200A are fixed at 90° to each other. Peak areas were taken as height × f.w.h.m. (full width at half maximum), and angular increments of 5° were generally used. For some of the vermiculite surfaces, however, an alternative and more expeditious technique for determining intensities as a function of angle was employed: the kinetic energies (k.e.) of the peak maxima, and the peak f.w.h.m., were identified from analogue scans and the count rates on each peak maximum and at background then obtained directly as a function of angle from the timer–scaler modules in the ES 200 instrumentation. Allowance had to be made when using this technique for the fact that the indicated peak positions changed by *ca.* 0.2 eV as the probe was rotated: this is, however, of no fundamental significance and probably reflects merely a variable dynamic surface charge (Evans 1977).

In some early experiments on the phlogopite and muscovite, peak intensities were obtained by using the digital recording and computer processing techniques described previously (Adams *et al.* 1977; Evans *et al.* 1977, 1978); while giving improved data quality, these techniques proved too slow to be employed throughout this work. Comparisons with the methods

described above confirmed that (within the increased error limits) the resultant peak intensity ratios were not dependent on the method of measurement.

The considerable body of data thus accumulated, comprising measurements of (usually) six peaks at seventeen angles for two or more specimens of each of five minerals, was then entered into computer files and the intensity ratio between each pair of peaks computed and plotted as a function of angle for each specimen. The variations with angle of those ratios conveying useful chemical information, normalized with respect to the mean ratio, comprise the X.p.d. patterns reproduced in § 3*c*. These mean intensity (area) ratios (i.e. in effect, the angle-integrated ratios) between each pair of elements were then used to obtain a quantitative chemical analysis of the region adjacent to each exposed cleavage, by using the technique previously established and evaluated for polycrystalline materials (Adams *et al.* 1977). For the high-magnesium minerals (phlogopite and vermiculite) a correction for the coincidence of the Bremsstrahlung-generated Mg KLL Auger signals with the Al 2s, 2p photoelectron peaks was applied, based on the measured intensity ratios between the Mg 2p and KLL Auger peaks in magnesium oxide. Because of the importance of ensuring that the reliability of the aluminium X.p.s. analysis was above suspicion – an importance which will become obvious later – measurements on phlogopite were undertaken with two X-ray targets, one containing about 10% aluminium and thus requiring a much larger correction term than the other. The analyses derived from the two sets of spectra were essentially identical.

Some intensity measurements were also conducted for series of cleaves through specimens of muscovite and phlogopite at constant electron takeoff angle: while accurate quantitative analyses cannot be obtained from such measurements (because diffraction effects are neglected), changes in an intensity ratio should still accurately reflect changes in the mineral composition as one proceeds through each sample.

The depth sampled in all these analyses depends on the escape depths for the photoelectrons concerned, which were therefore estimated for muscovite, by the 'intensity comparison' method previously described (Evans *et al.* 1977 and references therein). The absolute Si 2p (1144 eV) peak intensity from vacuum-cleaved muscovite was compared with the absolute intensity of the Au 4f signals from a layer of gold subsequently evaporated onto the muscovite surface in u.h.v. in the preparation chamber without breaking the vacuum. The gold layer was sufficiently thick to obscure completely the muscovite spectrum, and contamination levels on both surfaces were negligible. The peaks were recorded digitally and the areas determined by computer programme as previously described. The specimen was finally vacuum-cleaved a second time and the experiment repeated with a somewhat larger takeoff angle.

(*c*) *X-ray diffraction studies*

Representative cleaved flakes from each experiment were retained, following X.p.s. examination, for X-ray diffraction studies. They were mounted in a Weissenberg camera and the orientation of the rotation axis in the X.p.s. experiments determined (with respect to the principal symmetry axes of the generalized mica structure) by a Cu Kα oscillation photograph. The same samples of the vermiculite, both before and after Pb-exchange, were also examined on an X-ray diffractometer to determine their interlayer spacing(s).

(*d*) *Electron microscopic studies*

Small samples of muscovite, phlogopite, and the two synthetic hectorites were finely ground with acetone in an agate mortar, and each was introduced in turn into a Siemens Elmiskop 102 electron microscope fitted with a Link Systems 290 energy-dispersive X-ray analysis attachment. Copper grids were used, in the usual manner. Several small flakes (*ca.* 2000 Å) were selected in each case, and after their electron diffraction patterns had been visually checked, an energy-dispersive X-ray analysis was performed for each particle. When adequate signal/noise had been achieved, the cathode-ray tube display was photographed and the areas of the Mg, Al, Si, K and Fe Kα and of the Cu L peaks derived from tracings of the prints by cutting out and weighing each peak. Resolution of the curves into discrete peaks was carried out by visual estimation.

Because some spurious Al Kα intensity (and, to a much lesser extent, Fe Kα) was generated by X-ray excitation in some internal parts of the microscope close to the sample stage, a correction had to be applied to the measured intensities for these peaks. These corrections were derived from the mean of all the results for the synthetic hectorites, which contain no iron or aluminium, by assuming a linear relation between the Cu L intensity from the grid and the spurious Al and Fe signals. This is unlikely to be rigorously correct, but the residual error cannot be large as the total correction never exceeded about one-third of the detected Al Kα intensity. The consistency between net area ratios so obtained from different particles was always better than ±20% and usually ±10%: these figures naturally include the effects of any genuine variation of composition from particle to particle.

The results for muscovite (K, Si, Fe) and the hectorites (Mg, Si) were used to construct a Kα calibration graph (inverse relative sensitivity plotted against Kα X-ray energy), these materials being regarded as of known composition even on the micro-scale because (*a*) their bulk analyses agreed within error with the X.p.s. (surface) analyses and (*b*) the electron microscope results were consistent (10%) from flake to flake. A simple linear relation was assumed between the X-ray intensity from each element and the proportion of that element in the mineral. The graph was then used to derive relative atomic abundances for Si, Mg, Al, Fe and K in thin (*ca.* 1000 Å) flakes of the phlogopite from its X-ray spectra.

3. Results

(*a*) *Characterization and analyses*

The muscovite and lepidolite could be cleaved very readily by a razor blade to give high-quality mirror-smooth surfaces; the phlogopite and vermiculite somewhat less readily, leaving small visually-detectable irregularities in the exposed surfaces. Cleaved flakes of the lepidolite were almost colourless, with only a very pale pink tinge; those of muscovite were a light brown–green colour with, occasionally, small darker patches. The phlogopite and vermiculite both had rather more intense brownish colorations but could readily be differentiated, the phlogopite cleaving rather more readily, and into thinner, larger, flakes than the vermiculite. The crystallinity of the vermiculite flakes was noticeably affected by the ion-exchange treatment, which made them even more difficult to cleave successfully into large single flakes, and they retained a noticeable swelling (later confirmed by X-ray diffraction analysis, q.v.).

The analytical data obtained by the three techniques used are summarized in table 1.

Typical X-ray spectra obtained in the electron microscope are reproduced in figure 1: peak areas were converted to relative atomic abundances by multiplying by the following sensitivity factors, derived from the muscovite and hectorite spectra: 1.74 (Mg), 1.00 (Si), 1.14 (Al), 0.71 (K) and 0.69 (Fe). The cross section data and interpretative model used to convert X.p.s.

TABLE 1. COMPARISON OF MINERAL ANALYSES OBTAINED BY CHEMICAL, ELECTRON SPECTROSCOPIC, AND ELECTRON MICROSCOPIC METHODS

mineral	method	approximate effective sampling depth/Å	analysis results, reduced to atom ratios for comparability†	comments
muscovite	chemical	∞	$Si_{1.0}\ Al_{0.84}\ Mg_{0.05}\ Fe_{0.079}\ Ca_{0}\ F_{0.008}$	in satisfactory agreement (Si, Al)
	X.p.s.	10^2	$Si_{1.0}\ Al_{0.82}\ K_{0.25(4)}\ Na_{0.02-04}\ O_{4.37}$	
lepidolite	chemical	∞	$Si_{1.0}\ Al_{0.46}\ Mg_{0}\ Fe_{0.002}\ Ca_{0.008}\ F_{0.45(5)}$	in acceptable agreement (Si, Al, F)
	X.p.s.	10^2	$Si_{1.0}\ Al_{0.48}\ K_{0.25}\ Li_{0.40(8)}\ O_{3.4}\ F_{0.60(10)}$	
phlogopite	chemical	∞	$Si_{1.0}\ Al_{0.26}\ Mg_{0.89}\ Fe_{0.061}\ Ca_{0}\ F_{0.27}$	progressive increase in proportion of Al as sampling depth decreases
	e.m.	10^3	$Si_{1.0}\ Al_{0.32-0.46}$‡ $Mg_{0.81(9)}\ Fe_{0.067}\ K_{0.32}$	
	X.p.s.	10^2	$Si_{1.0}\ Al_{0.50}\ Mg_{0.60-73}\ K_{0.31(2)}\ Na_{0.01-03}\ O_{4.4}\ F_{0.26(3)}$	
vermiculite (natural)	chemical	∞	$Si_{1.0}\ Al_{0.36}\ Mg_{0.80}\ Fe_{0.17}\ Ca_{0.044}\ F_{0.026}$	see comment on phlogopite, above
	X.p.s.	10^2	$Si_{1.0}\ Al_{0.40-0.50}\ Mg_{0.73}\ Ca_{0.03-0.054}$§ $K_{0.1-0.18}\ O_{4.13}$	
vermiculite (Pb-exchanged)	X.p.s.	10^2	$Si_{1.0}\ Al_{0.56}\ Mg_{0.73}\ Pb_{0.21(2)}\ K_{0-0.05}\ O_{5.6}$	silicon, magnesium, and aluminium all invariant to ion-exchange

† X.p.s. and e.m. measurements cannot easily give absolute percentages of the elements present. X.p.s. analyses are reproducible to within 5% of the figures quoted except where indicated by an error limit for the last place (given in parentheses): an indicated *range* (in excess of the errors) reflects variation in the composition of the mineral from cleave to cleave. Note that not all elements were determined by all three methods: in particular alkali metals were determined only by X.p.s. because of the large excess of sodium present in the mineral solutions after dissolution via fusion with NaOH; in contrast Fe cannot be estimated by X.p.s. because of the frequent occurrence of multi-electron satellite peaks (see, for example, Evans *et al.* 1977), and was only determined by colorimetry and K-emission spectroscopy.

‡ Four microscopic flakes were analysed, and the range of the Al data considerably exceeded the experimental error revealed in the calibration data.

§ Ca and K vary inversely with each other from cleave to cleave. Total detected exchangeable ion was 0.21–0.24 equivalents (M^+) per Si at each cleave. Three surfaces were studied, cleaved *in vacuo* from two different flakes.

intensity ratios to relative atomic abundances have been fully described previously (Adams *et al.* 1977; Evans *et al.* 1977, 1978). Approximate X.p.s. analytical data for muscovite and phlogopite obtained from successive cleaves at constant take-off angle (the approximation resulting from the neglect of electron diffraction phenomena) are shown in figure 2: these illustrate the variability of the interlayer constituents in both minerals and of the principal octahedrally-coordinated element (Mg) in the phlogopite.

(*b*) *X.p.s. results*

Typical X.p.s. for each mineral are shown in figure 3 to complement the analytical data.

The intensity ratio Au 4f/Si 2p for peaks recorded under constant experimental conditions from closely-comparable clean surfaces of evaporated gold and vacuum-cleaved muscovite

respectively (as described in § 2), was 28.4 in the first such experiment and 36.1 in the second, for which the take-off angle was increased by 15°. Such variations are not unexpected, because the Si 2p intensity – derived from a single crystal – is modulated by diffraction effects whereas the gold 4f signal is not. We therefore take the mean value, 32.3, as the most appropriate for the estimation of the relative escape depths of these photoelectrons.

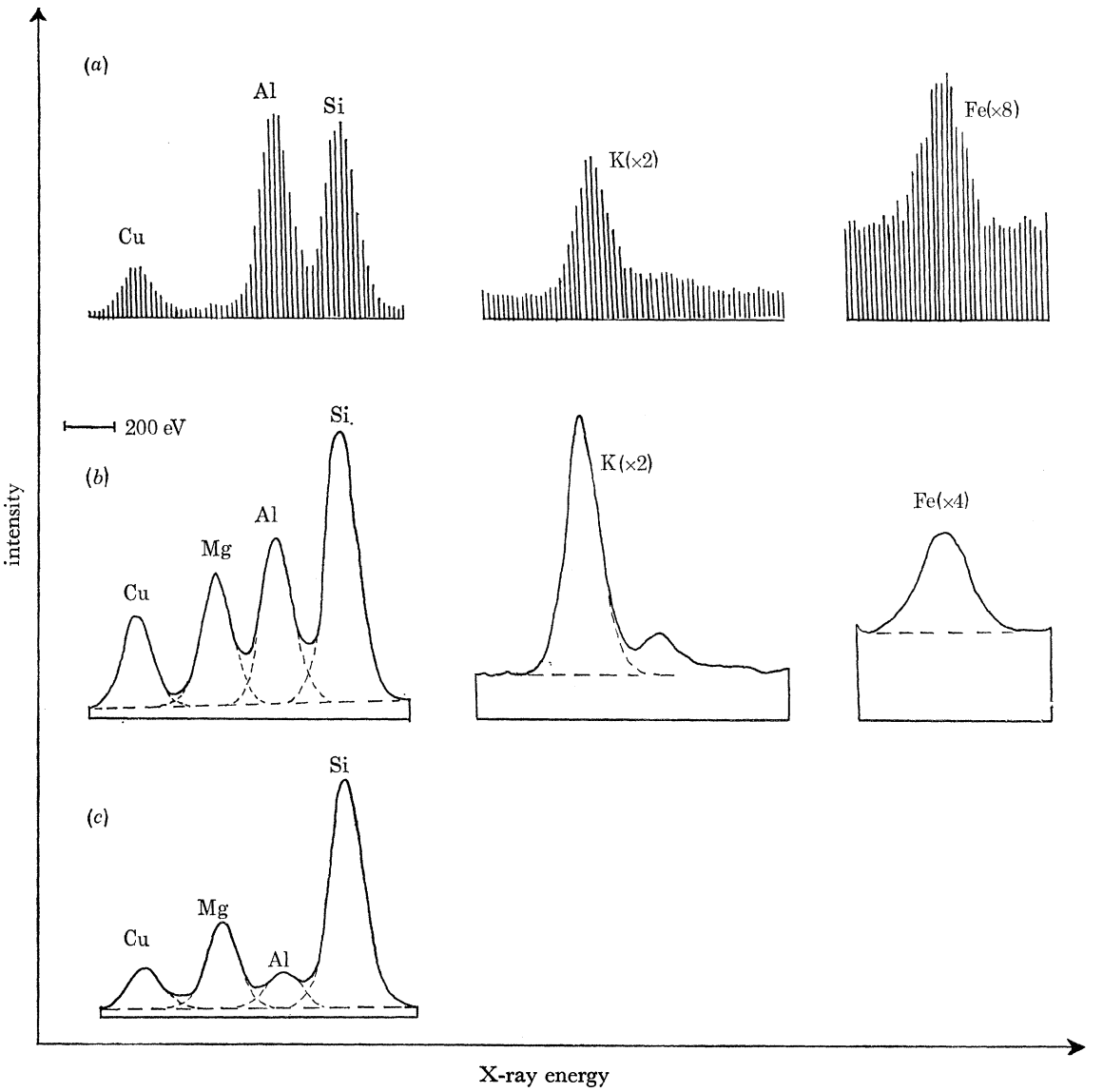

FIGURE 1. X-ray spectra obtained in the electron microscope from (*a*) muscovite (as photographed); (*b*) phlogopite and (*c*) a synthetic hectorite (laponite XLG) (peak envelopes showing estimated curve resolutions and background subtractions).

(*c*) *X-ray photoelectron diffraction patterns*

X.p.d. patterns for each mineral, derived from the raw spectra as described in § 5, are shown in figures 4–8. Lithium (1s) in lepidolite is not included in figure 6 because the limited data collected for this rather weak peak were found to be inadequate, the poor signal/noise ratio apparently resulting in a much wider random scatter than usual.

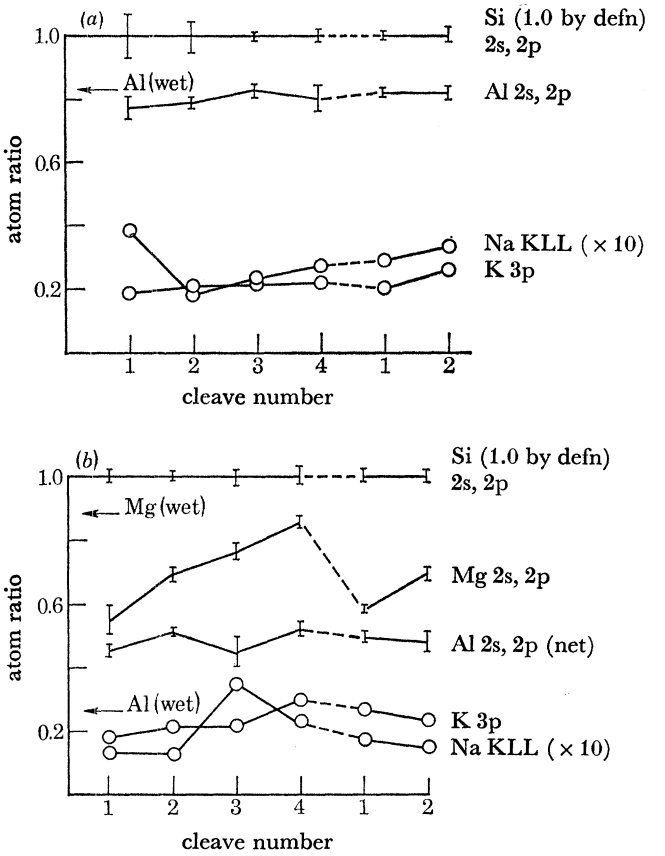

FIGURE 2. Variations in chemical composition over macroscopic distances as revealed by X.p.s. peak intensity ratios measured at fixed take-off angle. The ordinate is approximate ($\pm$ *ca.* 20 %) because electron diffraction effects are here neglected. The numerals on the abscissa relate qualitatively to depth: the first four cleaves in each case were taken over about 1 mm of the crystal, the subsequent 1, 2 referring to a second crystal. All cleavages were performed *in vacuo*. Bulk analyses for Mg and Al from table 1 are indicated by the word 'wet', with arrows, in each plot; (*a*) muscovite, (*b*) phlogopite.

(*d*) *X-ray diffraction data*

The basic structures of the minerals muscovite, phlogopite, lepidolite and vermiculite are closely related, and the principal axes of the unit cell in the plane of the silicate sheets may, somewhat loosely, be identified as an *a*-axis and two *a*-type axes, mutually at 120°, and similarly a *b* axis and two '*b*-type' axes located 30° from the '*a*-type' axes. The axes of rotation in the X.p.d. work, originally selected arbitrarily in order to obtain sufficiently large uniform rectangular surfaces for these experiments, were found to lie as shown in table 2.

TABLE 2. ROTATION AXES IN X.p.d. EXPERIMENTS

mineral	angle between rotation axis and *a*-type axis/deg†	angle between rotation axis and *b*-type axis/deg†
muscovite	8	22
phlogopite	14	16
lepidolite	24	6
vermiculite	21	9

† *a*-axis repeat distance *ca.* 5 Å. *b*-axis repeat distance *ca.* 9 Å.

PHILOSOPHICAL TRANSACTIONS OF THE ROYAL SOCIETY A MATHEMATICAL, PHYSICAL & ENGINEERING SCIENCES

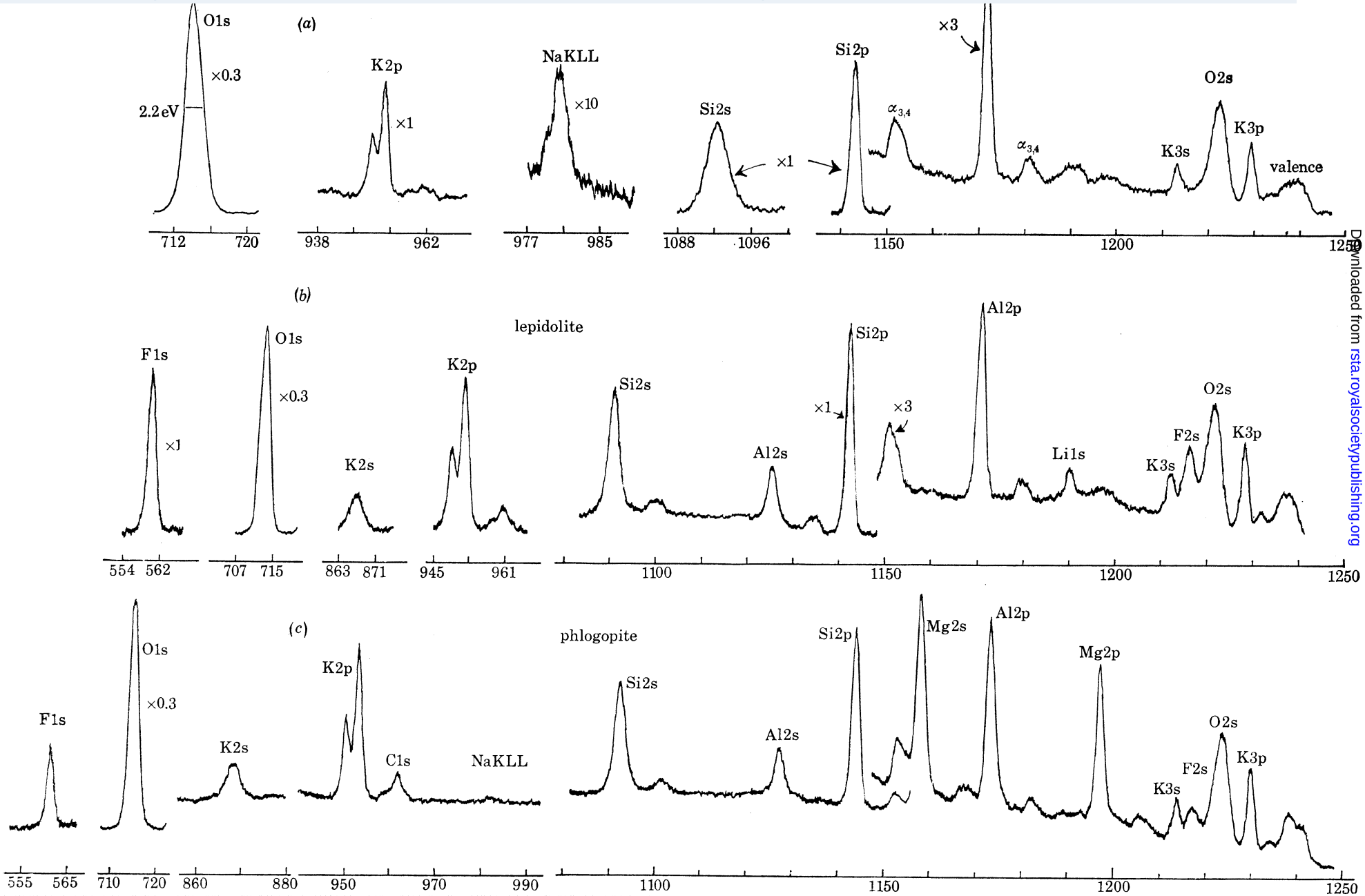

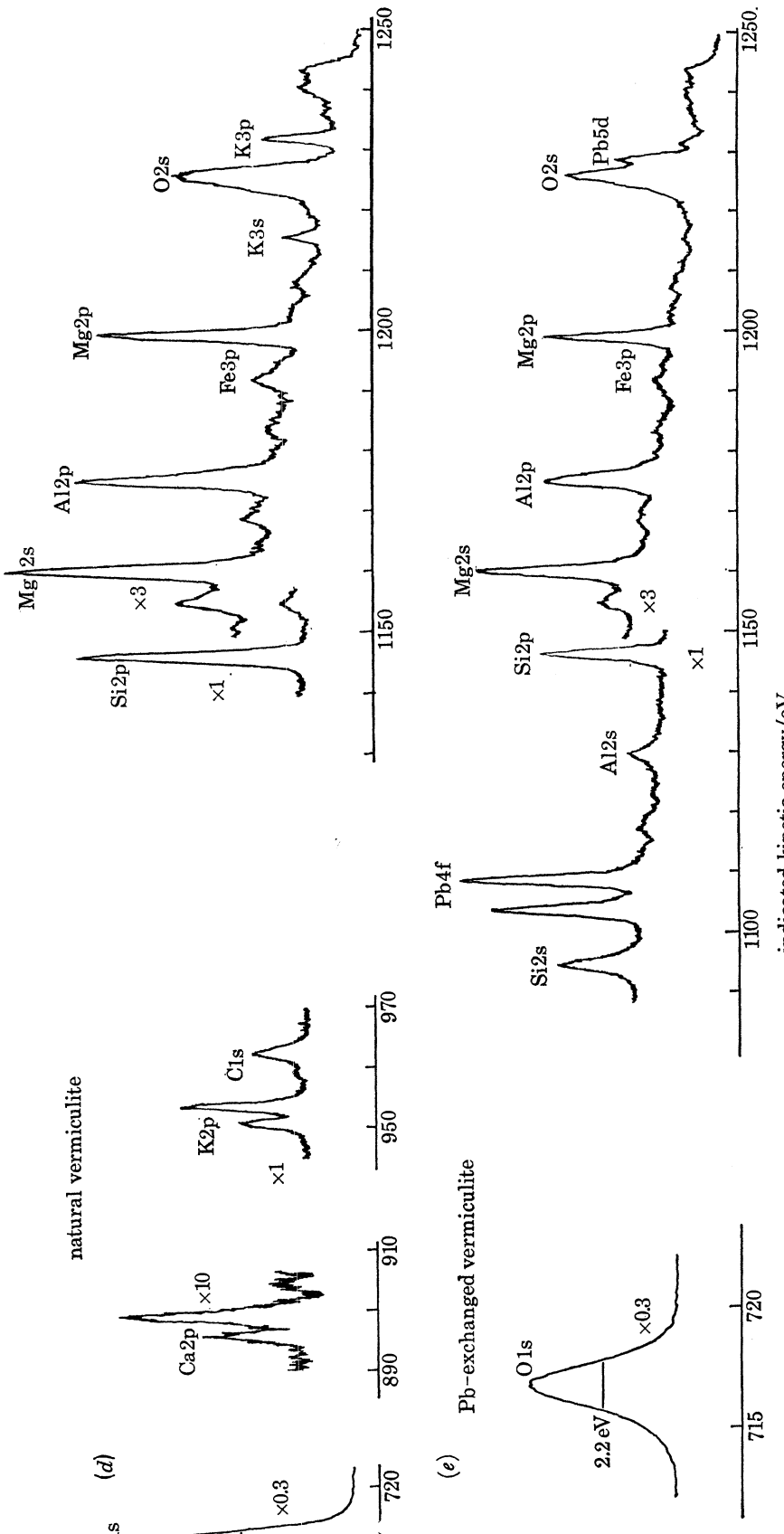

FIGURE 3. X.p.s. for muscovite, lepidolite, phlogopite, and natural and lead-exchanged vermiculites. Note that the scales for the lower-energy peaks (< 1100 eV) on the abscissa are not uniform – all the O 1s peaks, for example, are of comparable width. (*a*) Muscovite; (*b*) lepidolite; (*c*) phlogopite; (*d*) natural vermiculite; (*e*) Pb-exchanged vermiculite.

Bearing in mind that the angular resolution of the ES 200 is several degrees, the rotation axes of the muscovite and phlogopite samples, like those of the lepidolite and vermiculite flakes, may thus be regarded as essentially equivalent.

The repeat distance perpendicular to the silicate sheets in the natural vermiculite was found to be *ca.* 10.3 Å, although the diffractometer trace also revealed the presence of some 15.4 Å interlamellar spacings. Diffractometer studies of a lead-exchanged flake, however, showed an expanded layer spacing of *ca.* 12.4 Å throughout.

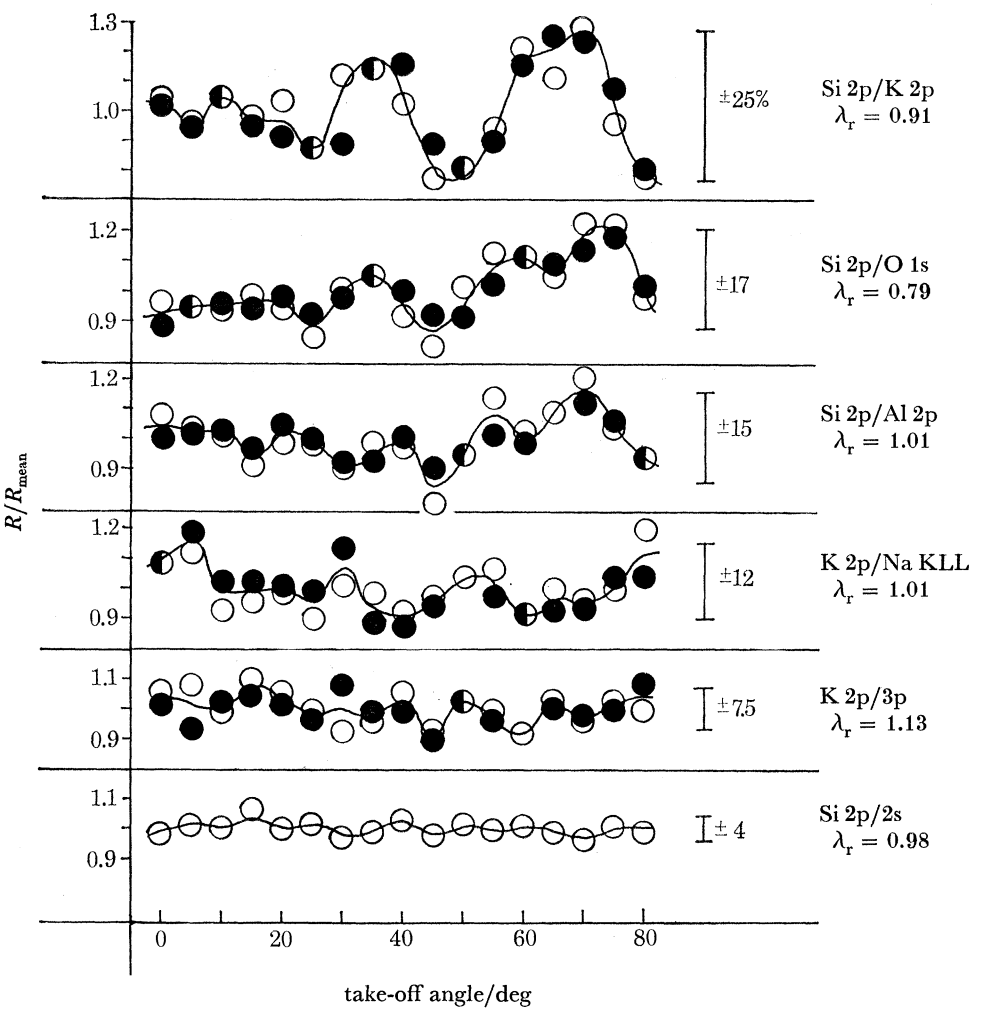

FIGURE 4. X.p.d. patterns for muscovite (two cleaves in one specimen, denoted by filled and open points). The take-off angle is defined as the angle between the electron beam and the normal to the sample surface. The symbol λ_r denotes the ratio of the de Broglie wavelengths of the photoelectrons concerned.

4. DISCUSSION

The principal innovation in the techniques of structural analysis employed in this work is the development and application of X-ray photoelectron diffraction as a tool for studying patterns of isomorphous substitution occurring in the outermost 100 Å or so of a complex single-crystal solid. We therefore describe first the principles involved in this new application

of angle-resolved X-ray photoelectron spectroscopy before proceeding to consider in turn all the data relevant to the structural chemistry of each mineral. In each case we have (i) endeavoured to establish satisfactory structural formulae both for the bulk mineral (via chemical analyses) and for the region adjacent to the cleavage planes (via X.p.s.), (ii) to elucidate the chemical significance of the X.p.d. patterns, and (iii) to seek explanations for the differences between the surface and bulk formulae which angle-resolved X.p.s. has enabled us to identify and quantify for the first time.

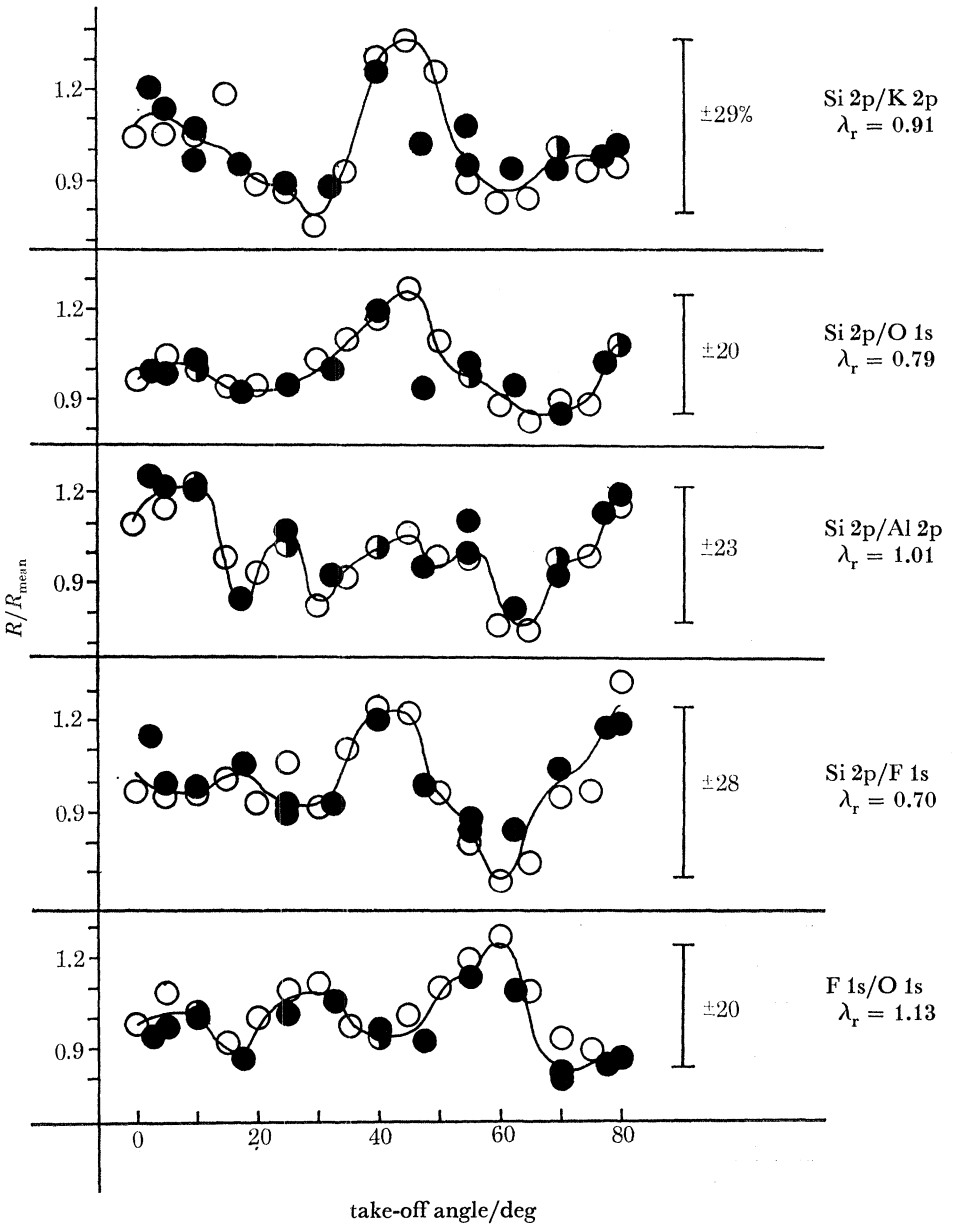

FIGURE 5. X.p.d. patterns for lepidolite (two cleaves in one specimen denoted by filled and open points); λ_r has the same significance as in figure 4.

(*a*) *Angle-resolved X.p.s. in structural analysis*

The angular variation of the *absolute* intensity of any core-level photoelectron peak is governed by a number of factors, not the least of which with most X.p.s. instruments are those relating to the experimental geometry. Even a small deviation of the axis of rotation from an ideal line located on the surface of the specimen and lying directly below the analyser entrance slit can cause a serious diminution of the signal as the electron take-off angle, θ, is increased†, as can electron 'shadowing' effects resulting from surface roughness in the specimens (Fadley 1976). However, all such incidental experimental variables cancel in the evaluation of the ratio between the intensities of any two signals generated under identical experimental conditions, and we shall consequently be concerned almost exclusively with the variation of intensity *ratios* with θ in the following discussion.

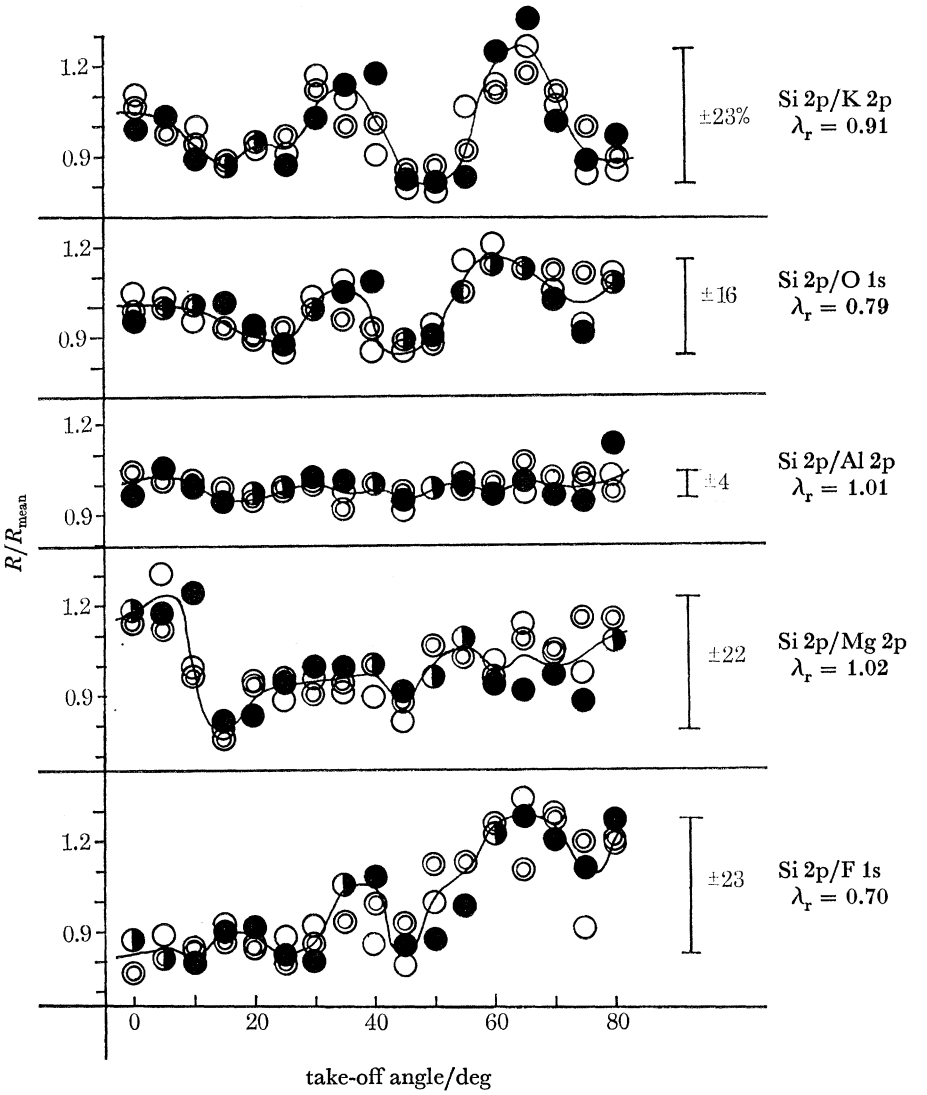

FIGURE 6. X.p.d. patterns for phlogopite (three cleaves in the same orientation distinguished by single circles, double circles, and solid circles).

† θ is defined throughout as the angle between the electron beam and the normal to the sample surface, and can in principle be varied between 0° (normal exit) and 90° (glancing exit).

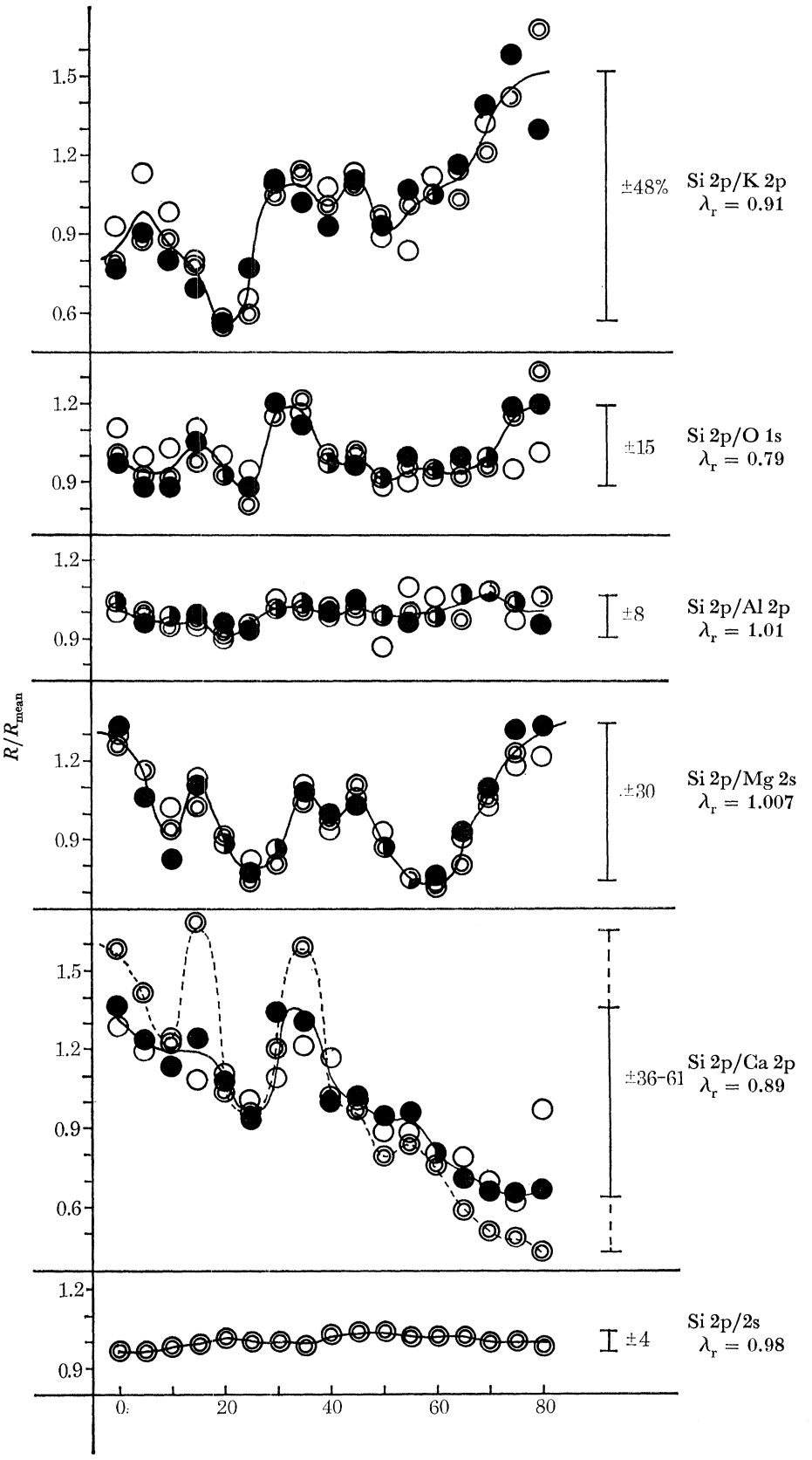

FIGURE 7. X.p.d. patterns for natural vermiculite (three cleaves, as in figure 6). The broken line for Si 2p/Ca 2p draws attention to the variability of the intensity of the diffraction maxima for Ca.

The ejection of photoelectrons from all filled (spherically symmetric) core shells is intrinsically isotropic in respect of the electron take-off angle, provided that the angle between the incident photons and the collected electrons is, as in almost all X.p.s. instruments, kept constant. Thus any peak intensity ratio obtained from a solid which is homogeneous throughout the sampling depth (and, in practice, clean polycrystalline specimens do seem to be effectively

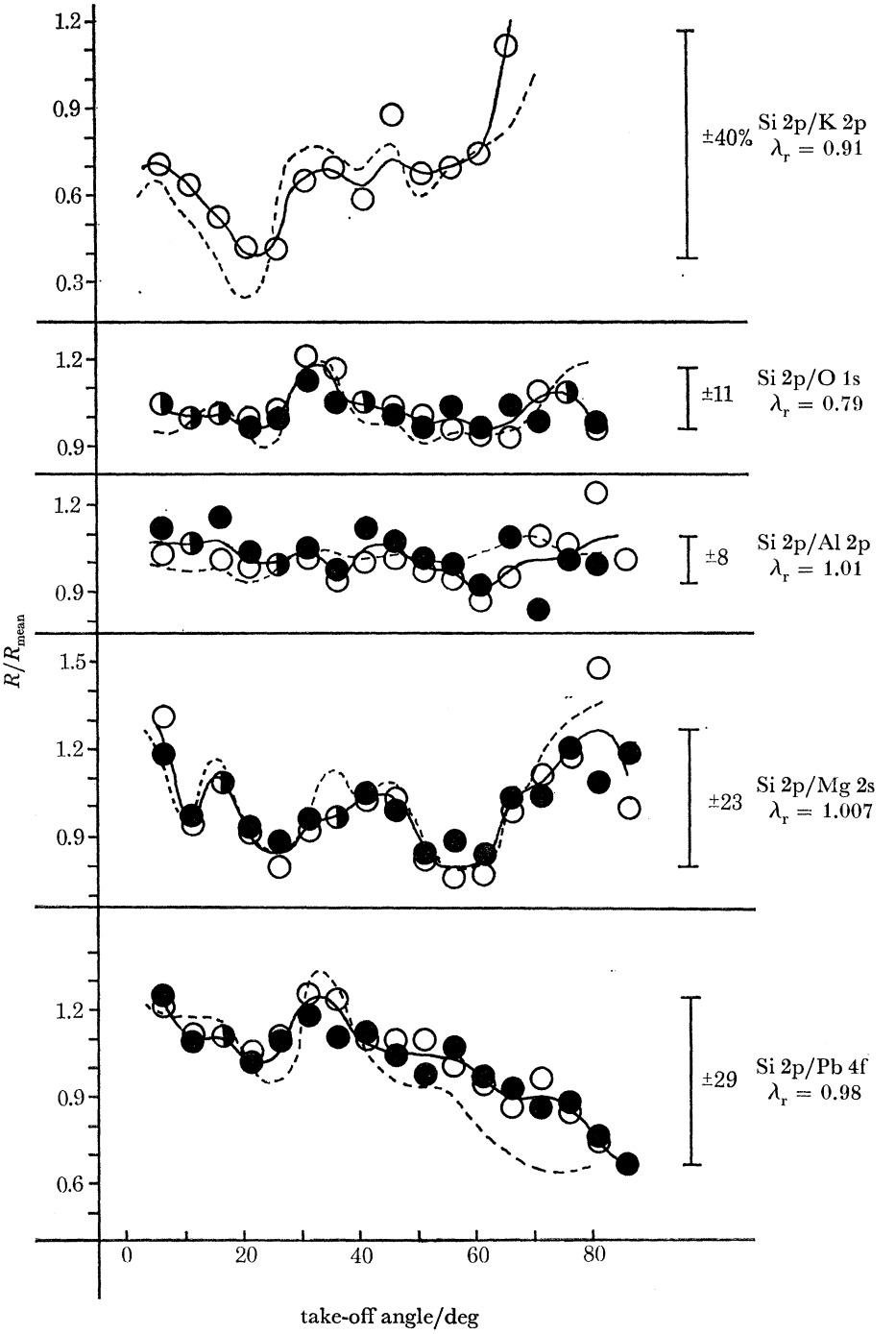

FIGURE 8. X.p.d. patterns for lead-exchanged vermiculite (two cleaves, filled and open circles). The broken lines follow the appropriate mean diffraction patterns from figure 7: for Si 2p/Pb 4f the full line for Si 2p/Ca 2p is adopted for comparison.

homogeneous) will be constant with respect to rotation of the sample; i.e. the X.p.d. pattern (plotted as in figures 4–8) will be a straight horizontal line. If, however, the element giving rise to one of the peaks exhibits a concentration gradient increasing towards the surface, the intensity of this peak will rise (relative to that of the other) as θ increases, because the effective sampling depth decreases with $\cos\theta$. Concentration gradients that are appreciable on an atomic scale can thus be readily detected, while if the functional form of the concentration gradient can be established, the X.p.s. data may be used to quantify the depth profile of the surface-enriched species (Evans 1978). Effects of this kind may be seen in the present work, superimposed on the diffraction patterns discussed below, in the Si 2p/K 2p, Si 2p/Ca 2p, and Si 2p/Pb 4f X.p.d. patterns for vermiculite (figures 7, 8), revealing potassium deficiency, but calcium or lead excess, in the surface region. Caution should however be exercised when the k.e. difference between the peaks compared is large, because any adventitious surface contamination will attenuate the low k.e. intensity by more than that at higher k.e. as θ increases (the sampling depth varying roughly as $(\text{k.e.})^{\frac{1}{2}}$): the upward trend of the Si 2p/F ls X.p.d. in phlogopite with θ (figure 6), where the k.e. difference is some 584 eV, is probably an instance of this.

In addition to all these effects, however, the photoelectron emission from single-crystal substrates always shows an oscillatory variation **in** intensity arising from diffraction of the outgoing photoelectrons by the ordered layer(s) of atoms at or near the surface of the specimen. For a fixed azimuthal orientation (i.e. specified experimental rotation axis) three factors might in principle be significant in governing the position and intensity of the diffraction maxima, namely (i) the location(s) of the emitting atoms within the solid, (ii) the de Broglie wavelength of the photoelectrons, and (iii) the radius of the ionized shell. However, since all the numerous intra-elemental intensity ratios examined have proved to exhibit only a minimal variation with angle (typically *ca.* $\pm 4\%$ for a close match in electron wavelength, e.g. Si 2p/2s in muscovite, rising only to $\pm 7.5\%$ for a 13% difference in wavelength, e.g. K 2p/3p in muscovite; see figure 4) the first factor, the atomic location, must dominate all others whenever the electron k.e. range involved is limited. Thus if two elements occupy equivalent sites in a single crystal, photoelectrons of comparable energies ejected from them will be diffracted into almost identical patterns, and the ratio between the two signal intensities will be invariant with θ. An excellent example of this is seen in the Si 2p/Al 2p ratio for phlogopite (figure 6). Conversely, if two elements are confined to unique and different sites, the ratio of their peak intensities will show a maximal variation with θ, generally of the order of 25–30% in the minerals studied here. The presence of a fraction of one element in sites typical of the other, or of one element in multiple sites, will reduce the range of variation observed: oxygen for example is found in three distinct environments in micas and the Si 2p/O 1s X.p.d. patterns reflect this with ranges of 11–20%. Inspection of the *individual* intensities in this case (not illustrated) reveals that, predictably, the oscillatory variation of the O 1s signal is much less marked than that of the Si 2p peak.

The absolute magnitudes of the ranges as measured depend, however, not only on the fundamental factors discussed above but also on the angular resolution of the instrument employed (and, more subtly, on the angular increment used in recording the patterns: some preliminary data collected with 15° increments revealed little more than half the true range) and on the nature and quality of the crystal. The sample area required is relatively large (*ca.* 1 cm^2) and appreciable polycrystallinity might seriously reduce the observed ranges. However, the ranges

PHILOSOPHICAL TRANSACTIONS OF THE ROYAL SOCIETY A MATHEMATICAL, PHYSICAL & ENGINEERING SCIENCES

apparent in the data reported by Siegbahn *et al.* (1970) (for sodium chloride) and by Fadley (1976) (for gold and silicon) suggest that our figures may be typical of many samples and instruments.

Finally, we may remark that all the foregoing arguments apply equally to photon-excited Auger spectra, so that the Auger peaks that appear in most X-ray photoelectron spectra may be used interchangeably with the photoelectron peaks for X.p.d. purposes. This may often be advantageous as an Auger signal is frequently much more intense than any of the photoelectron peaks in the relevant k.e. region, for example the principal Na KLL Auger line has an 'effective cross section' an order of magnitude larger than that of either Na 2s or 2p (see § 4(*c*)). (Adams *et al.* 1977).

(*b*) *Structural formulae*

The formulae proposed in the following sections are given according to the usual convention, as illustrated below:

$$\overbrace{M^{I}}^{\text{interlayer cation(s)}}\ \overbrace{[M_2^{III}]}^{\text{octahedrally-coordinated cations}}\ \overbrace{[M_3^{IV}\,M_1^{III}]}^{\text{tetrahedrally-coordinated cations}}\ \overbrace{O_{10}\,(OH,\,F)_2}^{\text{structural anions}}$$

The totals of ions as given within the square brackets in the following sections occasionally deviate slightly (0.01) from the ideal formulae because of rounding-off errors in their evaluation. (The reproducibility of the analytical data from sample to sample does not justify the retention of three decimal places.) A comprehensive introduction to the structural chemistry of the sheet silicate minerals has been given by Deer *et al.* (1962).

(*c*) *Muscovite*

The idealized formula for this mineral is $K[Al_2]\,[Si_3Al]\,O_{10}(OH)_2$, illustrated in figure 9. The (variable) substitution of Al for Si in the tetrahedral sites is believed to be the main source of the layer charge, although the replacement of some of the octahedral Al^{III} by Mg^{II} or Fe^{II} can also contribute. Substitution of octahedral Al^{III} by Fe^{III} is possible but does not affect the layer charge. If a parameter x is introduced to characterize the extent of tetrahedral substitution, together with a second parameter y related to the extent of octahedral substitution, and the formula is renormalized to $Si_{1.00}$ to facilitate comparison with the data of table 1, we can write a general formula for this mineral as

$$M^{I}_{(x+y)/(4-x)}\,[M^{III}_{(2-y)/(4-x)}\,M^{II}_{y/(4-x)}]\,[Si_{1.0}\,M^{III}_{x/(4-x)}]\,O_{10/(4-x)}(OH,\,F)_{2/(4-x)}. \qquad (1)$$

From the summation of the chemical analyses for Al, Fe and Mg, we find $x = 0.95$; consideration of the total detected interlayer ions in the X.p.s. analyses (which do not differ significantly from the bulk analyses where comparison is possible) suggests that y should be chosen as small as possible consistent with the Mg analysis. We therefore assume that the small quantity of Fe present is predominantly Fe^{III}, and set $y = 0.15$. This yields a structural formula

$$M^{I}_{0.36}[Al_{0.53}\,Fe^{III}_{0.08}\,Mg_{0.05}]\,[Si_{1.0}\,Al_{0.31}]\,O_{3.28}(OH)_{0.649}\,F_{0.008}, \qquad (2)$$

or, with the more usual normalization,

$$M^{I}_{1.1}[Al_{1.62}\,Fe^{III}_{0.24}\,Mg_{0.15}]\,[Si_{3.05}\,Al_{0.95}]\,O_{10}(OH)_{1.98}\,F_{0.02}. \qquad (2a)$$

Comparing (2) with the X.p.s. analysis in table 1 we do not find any convincing evidence for compositional differences between the cleavage planes and the bulk material. The total interlayer ion content should, apparently, be somewhat higher than that implied by the X.p.s. results (0.36 per Si cf. *ca.* 0.31 for maximum Na + K by X.p.s.), but it seems plausible to attribute this difference to the presence of small quantities of other ions (Li, Cs, Rb), each of which individually lies below the X.p.s. detection limit (cf. F, here detected by chemical techniques but not by X.p.s.). The total oxygen content obtained by the rationalization procedure (3.93 per Si) is reasonably consistent with the X.p.s. value (4.37), which has an estimated probable error of the order of 10 % because of the large k.e. difference between the cation peaks and the O 1s peak.

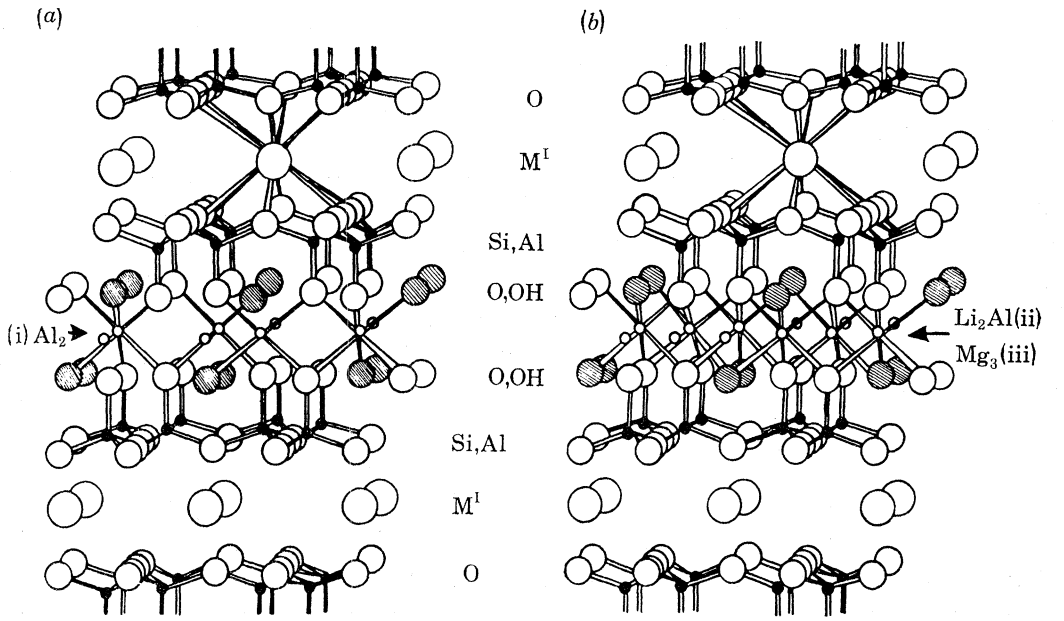

FIGURE 9. Generalized structures for micas and related minerals: (*a*) dioctahedral ((i) muscovite), (*b*) trioctahedral ((ii) lepidolite; (iii) phlogopite and vermiculite). The interlayer ion may be hydrated in vermiculites (not shown).

Turning to the X.p.d. data for this mineral, we find the overall ranges for K, Si, O and Al shown in figure 4 to be fully consistent with the structure deduced above. The widest range of variation is 25 % (for Si/K ratios) confirming that these elements are located at different unique sites, while a somewhat lower range is evident when one element occupies more than one site (Si/O, 17 %; Si/Al, 15 %). The 40 % reduction in range from Si/K to Si/Al is closely paralleled by the 37 % of the aluminium which is postulated (by formula (2) above) – and quite independently of the X.p.d. data – to be in tetrahedral (silicon) sites.

The X.p.d. data for sodium (K/Na), however, provide us with new structural information. This X.p.d. range significantly exceeds that expected for simple isomorphous substitution (*ca.* 4 %, as for intra-elemental ratios for peaks close in k.e.) and that this is not simply attributable to inadequate counting statistics is shown by the consistency of the pattern from cleave to cleave. However, the range for K/Na is nowhere near as large as for Si/K, and it seems that the sodium and potassium ions must occupy nearly, but not exactly, equivalent sites in the muscovite structure. This conclusion cannot be verified by conventional diffraction techniques for the

determination of crystal structure because the sodium comprises only about one-tenth of the interlayer ion (table 1), randomly distributed throughout the sampling depth, and silicates with such high layer charge do not generally undergo ion-exchange reactions. The only reliable techniques in such circumstances are those in which – as in X.p.d. and e.X.a.f.s. – the data relating to the separate elements are obtained independently, rather than collectively. However, studies of the interlayer crystallography as a function of exchangeable ion have been conducted on the closely related mineral montmorillonite, by Pezerat & Méring (1967), who found that the smaller sodium ion prefers an off-centre site between the aluminosilicate layers in that mineral, thus optimizing its coordination to an oxide hexagon on the face of one layer, whereas the larger potassium ion is indeed located midway between the layers, enjoying an enhanced coordination number with, ideally, twelve nearest neighbours. The operation of an analogous displacement for interlayer sodium in muscovite would account very convincingly for the X.p.d. data in this case, and it had previously been pointed out (Gruner 1942) that the small ionic size of sodium made it less appropriate than potassium for the interlayer sites with twelve-fold coordination.

Having established a reliable total structural formula for this muscovite, we now turn to the intensity comparison described in §§ 2(*b*) and 3(*b*) to derive a figure for the inelastic mean free path, λ, of *ca.* 1144 eV electrons in this mineral, by using the method described in detail by Evans *et al.* (1977). Taking the value for 4f photoelectrons in gold as 14 Å, we obtain a value of 34.5 ± 4 Å, very close to the best recent determinations for silica (37 ± 4 Å at 1382 eV, implying *ca.* 34 Å at 1144 eV) by Hill *et al.* (1976). In view of the close similarity in structure between all the minerals studied, such a figure may consequently reasonably be applied in consideration of all the X.p.s. analyses described in this paper. The effective total sampling depth (*ca.* 3λ) thus varies from *ca.* 100 Å at $\theta = 0°$ to *ca.* 17 Å at $\theta = 80°$ for the faster photoelectrons, reducing to 70–80 % of these figures for the slower electrons ejected from the O 1s and F 1s levels. Where no near-surface concentration gradients are apparent from the X.p.d. the X.p.s. analyses thus relate overall to the outermost ten aluminosilicate layers, although, because of the exponential weighting of the measurements towards the surface, they do also indicate with considerable reliability the composition of the outermost (exposed) layer.

(*d*) *Lepidolite*

Lepidolite is a trioctahedral mica, of ideal formula $K[Li_2Al]\,[Si_4]O_{10}(OH, F)_2$ (figure 9). The layer charge is thought to derive essentially not from the substitution of trivalent ions into the tetrahedral sites – though in practice some such substitution does occur – but from the replacement of octahedrally-coordinated Al^{III} in the idealised muscovite structure (figure 9) by twice their number of Li^{I} species. In the limiting (ideal) case, all the octahedral sites are thus occupied, half the aluminium having been replaced.

Introducing adjustable parameters x and y into the ideal formula to characterize variable isomorphous substitutions, as before, we first obtain the general formula

$$M^{I}_{(x+y)/(4-x)}\,[Li_{2y/(4-x)}Al_{(2-y)/(4-x)}]\,[Si_{1.0}Al_{x/(4-x)}]\,O_{10/(4-x)}(OH, F)_{2/(4-x)}. \qquad (3)$$

In this case the magnesium, calcium and iron contents are negligible, and a comparison of the X.p.s. and bulk analyses in table 1 does not reveal any significant differences. The fluoride content suggested by X.p.s. is appreciably higher than the bulk analysis figure, but considering the large k.e. difference between the F 1s and the reference Si 2p line, this discrepancy should

rather be regarded as within the combined possible error limits, especially when the oxygen data are also considered (see below). Since this material thus apparently cleaves in regions of typical composition, we may combine the bulk and X.p.s. analyses to characterize in detail its substitutional patterns. Two sets of simultaneous equations in x, y can be obtained by using the aluminium figures in combination with the X.p.s. data for either potassium *or* lithium, leading to structural formulae in the range

$$K_{0.25-0.31}[Li_{0.33-0.40}Al_{0.35-39}]\ [Si_{1.0}Al_{0.08-0.11}]\ O_{2.71-77}(OH)_{0-0.1}F_{0.45-55}, \tag{4}$$

or, renormalized to the oxygen content,

$$K_{0.92-1.12}[Li_{1.22-44}Al_{1.26-40}]\ [Si_{3.61-69}Al_{0.30-40}]\ O_{10}(OH)_{0-0.36}F_{1.63-98}, \tag{4a}$$

where the higher lithium contents imply both the higher potassium figures and the greater degree of substitution by aluminium in the tetrahedral sites. We prefer the high-Li formulation on the grounds that as the experimental cross section used to obtain the Li analysis is much more likely to be too high than too low (see Evans *et al.* 1978) our lithium analysis should be taken as approximating to a lower, rather than an upper, limit. It thus seems probable that in this case, as with muscovite, traces of other undetected species make up the balance of the interlayer ions.

Again, as with muscovite, the X.p.d. data fully support the above structure. Where the sites of the emitting atoms are unique and distinct (Si/K, Si/F) the ranges of variation are maximal (28–29%), reducing to 23% for Si/Al where partial cancellation of the pattern would be expected. The reduction in range (*ca.* 21% of the total) again parallels closely the 17–24% of the aluminium that was independently deduced above as occupying tetrahedral sites. The X.p.d. results for Si/O and O/F are likewise entirely consistent with the several distinct oxygen sites expected, the variation of the latter ratio confirming that fluoride cannot substitute randomly for oxygen but must replace one component – presumably hydroxyl – preferentially.

The oxygen X.p.s. analysis is *ca.* 20% higher than that given by formula (4), but in view of the similarly high results given by the F 1s signals at *ca.* 160 eV lower k.e. (discussed earlier) we think this is unlikely to be compositionally significant: certainly any increase in oxygen content even approaching 20% would be very difficult to accommodate within the established structure. A similar, though less marked, overestimation of the oxygen content has already been noted for the muscovite, but such effects are not obvious in the data for the phlogopite or the vermiculite (q.v.). The origins of this systematic, but apparently specimen-dependent, overestimation of elements determined via low k.e. peaks remain obscure: other recent work (Madey *et al.* 1977; Powell 1978) also suggests that unrecognized factors may be important in quantitative applications of X.p.s. where large k.e. differences are involved.

(*e*) *Phlogopite*

Phlogopite is generally regarded as a trioctahedral mica, of ideal formula $K[Mg_3]\ [Si_3Al]\ O_{10}(OH, F)_2$, illustrated in figure 9. As in muscovite, the layer charge is governed principally by the extent to which trivalent aluminium replaces tetravalent silicon in the tetrahedral sites, although the substitution of trivalent (or, less commonly, monovalent) cations for a fraction of the octahedral magnesium is also thought to be significant. However, as the only monovalent ion generally considered small enough to be readily accepted into the octahedral sites is lithium, and we have positive evidence for the absence of any significant lithium content, we shall

initially neglect the possibility of monovalent octahedral substitution. Introducing parameters x and y as before, we have therefore

$$M^{I}_{(x-y)/(4-x)}[M^{II}_{(3-y)/(4-x)}M^{III}_{y/(4-x)}]\ [Si_{1.0}M^{III}_{x/(4-x)}]\ O_{10/(4-x)}(OH,\ F)_{2/(4-x)}. \tag{5}$$

From the chemical analyses for Mg, Fe and Al, taken together, we find $x = 0.83$, which in turn permits a maximum trivalent tetrahedral occupation of 0.26 per Si. Since this is precisely the figure obtained by analysis for (bulk) aluminium, and bearing in mind that the X.p.d. data confirm that the aluminium and silicon occupy equivalent sites despite the higher aluminium content reflected in the X.p.s. analyses (see below), we conclude that there is no octahedral aluminium, and, as expected, no tetrahedral Fe^{III} in these specimens. In the octahedral sites, the oxidation state of the iron is uncertain, leading to limiting structural formulae

$$M^{I}_{0.20-26}[Mg_{0.89}Fe^{II-III}_{0.06}]\ [Si_{1.0}Al_{0.26}]\ O_{3.16}(OH)_{0.36}F_{0.27}, \tag{6}$$

$$M^{I}_{0.63-82}[Mg_{2.82}Fe^{II-III}_{0.19}]\ [Si_{3.16}Al_{0.83}]\ O_{10}(OH)_{1.14}F_{0.85}, \tag{6a}$$

the lower interlayer ion content naturally corresponding with the higher oxidation state for the iron (cf. (5)).

These formulae are however definitely not consistent with the X.p.s.-derived surface analysis (table 1). Relative to silicon, the near-cleavage regions in this phlogopite contain almost twice the aluminium content of the bulk mineral, and are significantly deficient in magnesium. The X.p.s.-detected interlayer ion content is here greater than that required by (6) (the inverse of the situation for muscovite and lepidolite), while the oxygen content (but, significantly, not that of fluoride) suggested by X.p.s. is again seriously high. These regions are clearly not typical of the bulk mineral, yet a reasonably reproducible X.p.s. analysis is given by all fourteen cleavage surfaces examined. The variation in composition from cleave to cleave (figure 2) is significant, but much less, particularly in the aluminium content, than the difference between bulk and surface.

These differences cannot be attributed simply to a lack of adequate angular averaging in the X.p.s. analyses; the Si and Al peaks show essentially the same angular behaviour (figure 6), an observation that confirms that all the excess aluminium is in substitution for silicon. This fact also eliminates the other obvious trivial explanation, i.e. that the small correction for the coincidence of Al 2p and Mg KLL signals might have been grossly insufficient. This question has already been considered in § 2: it suffices here merely to add that if Mg-derived electrons were to contribute to any extent to the Al 2p peak height, an X.p.d. range for Si 2p/Al 2p as low as that for Si 2p/2s could not have been obtained. Mg and Si occupy totally distinct sites, an expectation confirmed by the Si 2p/Mg 2p X.p.d. range of 23%, the highest observed in phlogopite.

We have therefore to rationalize the observed surface analysis in terms of possible modified structural formulae. The Al/Si ratio of 0.50 enables us to deduce (from (5)) that here $x = 1.33$, and if we accept the X.p.s. total for interlayer ion content (*ca.* 0.33 per Si) we have $y = 0.45$ and a formula

$$M^{I}_{0.33}[M^{II}_{0.95}M^{III}_{0.17}]\ [Si_{1.0}Al_{0.50}]\ O_{3.74}(OH)_{0.49}F_{0.26}. \tag{7}$$

Now, however, we have an apparent octahedral M^{III} content about three times the known bulk iron content, with the X.p.d. result excluding the participation of Al^{III} here. Moreover,

although the predicted oxygen content matches the X.p.s. much better than before, the M^{II} prediction still considerably exceeds that detected (0.95 per Si, cf. 0.60–0.73 for Mg). Be^{II}, like Li^{I}, would be sufficiently small to replace Mg^{II} in isomorphous substitution and is, on an equivalence basis, equally difficult to detect by X.p.s.: but a proportion of beryllium sufficient to resolve the present difficulty would, without doubt, have been detected. We are thus forced to conclude that there must be a very significant deviation from the accepted phlogopite structure in regions of facile cleavage.

Nevertheless, the similarity between the Si 2p/K 2p and Si 2p/O 1s X.p.d. patterns for muscovite and phlogopite, recorded for roughly equivalent axes of rotation (table 2), suggests that these elements at least are similarly located in the two minerals, and so we seek a rationalization that retains the established basic structure as far as possible. One cannot, however, postulate that many of the octahedral sites simply remain unoccupied, because this would drastically increase the layer charge and inhibit, rather than facilitate, cleavage. But if, in addition, numerous concomitant oxide vacancies were to be accepted, or, perhaps more plausibly, about one-fifth of the oxide ions were to be replaced by hydroxyl (i.e. were protonated), the X.p.s. analyses could be understood in terms of structures reminiscent of a dioctahedral mica: about one-third of the octahedral sites would in this model remain vacant. Comparison of the X.p.d. pattern for Si/Mg in phlogopite with that for Si/Al in muscovite reveals little obvious resemblance of even a qualitative nature, and given that the Si, K and O X.p.d. data match well between the two minerals, this does imply a significant distinction between the respective Mg and Al sites.

Alternative possibilities in which the layer charge would be minimized by substantial loss of hydroxyl seem less convincing because the surface fluoride content (isomorphous with hydroxyl) is not anomalous. Moreover, the replacement of lattice oxide by hydroxide in montmorillonite – though with a concomitant reduction in silicon content rather than in that of the octahedral ions – has previously been postulated by McConnell (1950), and it is well established that in biotite (a trioctahedral mica closely related to phlogopite) the (bulk) octahedral ion content frequently falls well below that expected (see, for example, Deer *et al.* 1962).

This picture is, however, further complicated by the possible introduction of monovalent ions to take up the vacant octahedral sites. One initially attractive hypothesis – that H_3O^+ ions occupy some of the octahedral sites – should probably be discarded in view of the large size of this ion (effective radii: H_3O^+, *ca.* 1.1–1.2 Å; Li^+, 0.60 Å; Mg^{2+}, 0.65 Å; Al^{3+}, 0.50 Å): the lack of any detectable chemically-shifted O 1s signal (figure 3) also militates against this possibility. The presence of additional H^+, relying on the lattice oxide and hydroxide for solvation, cannot, however, be easily disproved (or confirmed) and must remain a speculative possibility.

It is remarkable that the structural modifications we have tentatively identified above apparently cause phlogopite to cleave so much more readily in the regions affected that not even one cleavage typical of the bulk was obtained. As we have shown, there is no evidence for a reduction in layer charge in these regions, and it would seem that strains, and possibly consequent distortions of the layers from planarity, resulting from the abnormal substitution patterns, are probably the major cause. Dioctahedral micas in general are believed to be more distorted from their ideal structures than are their trioctahedral counterparts (Deer *et al.* 1962). Another relevant factor, recently investigated theoretically in some detail, is the possible role

of fluoride substitution in the determination of cleavage energies in micas (Giese 1978). The calculations, however, suggest that the fully fluoride-substituted structure should be only marginally more difficult to cleave than the normal mica, which is in agreement with our experimental result to the extent that the fluoride content is not atypical near a cleavage plane: but no positive effects due to the presence of fluoride are apparent.

Finally, we discuss the interrelation between the surface and bulk structures as elucidated above. Neither the Si/Al nor the Si/Mg X.p.d. patterns shows any progressive mean trend with increasing θ (decreasing effective escape depth); thus we may be confident that the compositional differences extend over at least 100 Å before reapproaching the bulk composition. At what depth, then, is the bulk structure regained? The e.m. measurements summarized in table 1 enable us to suggest that these compositional variations in fact extend over depths of the order of 500–1000 Å, because 1000 Å is the depth typically sampled in transmission e.m., and the derived mean compositions (for Si/Al, Si/Mg) lie intermediate between the X.p.s. and bulk chemical analyses. However, the errors in quantitative e.m. analysis by this technique are relatively large and have not yet been adequately studied. In our approach to calibration, no explicit corrections comparable with the 'ZAF' scheme for the electron microprobe (see, for example, Dunham and Wilkinson, 1978) are applied. Indeed, no system yet exists for applying such corrections in the present context when the sample is not of effectively infinite thickness. However, it seems reasonable that when calibration is undertaken with materials closely similar both structurally and chemically to the unknown, these corrections may be assumed to cancel.

Subsequent to the experiments described here, the microscope has been modified to move the X-ray detector much closer to the sample and so eliminate the spurious Al and Fe signals mentioned in § 2: a much more extensive calibration procedure has now also been carried out, one which does not employ mineral standards (Crawford 1978; Crawford & Jefferson, in preparation), and the differences between the derived calibration factors from the two studies are not large enough to invalidate the conclusions outlined above. Indeed, further e.m. studies of this phlogopite by Crawford (1978) have given analyses close to those we report (mean: $Si_{1.0}Al_{0.42}Fe_{0.076}Mg_{1.0}$).

The overall picture is thus one in which the composition of this mineral varies in respect to its aluminium content in a cyclic fashion, the separation of maxima and minima being of the order of hundreds of Å. Changes in the magnesium content also occur, but over much larger depths, of the order of about a millimetre. Compositional changes from one layer to another seem always rather small, not being large enough to cause any noticeable perturbation of the X.p.d. patterns. However, it appears that cleavage occurs preferentially in regions of high aluminium content, and in which the aluminium is still entirely tetrahedrally coordinated. A substantial number of octahedral vacancies, possibly protonated, are also proposed, accompanied by defects in the oxygen structures to avoid any concomitant drastic increase in the local layer charge.

(*f*) *Vermiculite*

Idealized trioctahedral vermiculite is in essence a mica of the phlogopite type, but with a significantly reduced layer charge permitting *hydrated* ions, generally magnesium, to enter the interlayer region. A typical formula would be

$$Mg_{0.25}(H_2O)_{1.5}[Mg_3]\ [Si_{3.5}Al_{0.5}]\ O_{10}(OH, F)_2. \qquad (8)$$

Nevertheless, our experience with minerals supplied as vermiculite has been that many specimens as received contain potassium as a principal interlayer ion, which X-ray diffractometer studies suggest is largely anhydrous. Since it is generally possible to exchange the interlayer ion in vermiculites, we thus felt it would be particularly valuable in studies of the structural chemistry if complementary data before and after ion-exchange were acquired.

Indeed, the derivation of a basic structural formula for the material studied here is considerably simplified if certain aspects of the ion-exchange experiment are considered first. The X.p.s. analyses in table 1 show clearly that aluminium *and magnesium* are not reduced in abundance relative to silicon by prolonged refluxing with lead nitrate solution, so that these must be the structural cations, while calcium and potassium are the principal natural exchangeable cations. With due allowance for the existence of divalent, possibly hydrated, interlayer ions, general formula (5) above may then be applied: comparison of total bulk chemical analyses for magnesium, iron and aluminium then yields $x = 1.00$, enabling us to establish the tetrahedral M^{III} content as 0.33 atoms per Si. If, as expected on chemical grounds, this is all aluminium, there must be 0.03 Al per Si in octahedral sites: this conclusion is consistent with the X.p.d. for Si/Al which shows a range (8%, see figures 7, 8) not greatly increased from the 4% typical of complete isomorphous replacement (as, for example, in phlogopite), even though the X.p.s. *analysis* (which we discuss below) is not in agreement with the bulk analysis. We thus obtain basic structural formulae for the bulk mineral (neglecting interlayer hydration) in the ranges:

$$Ca_{0.044}M^{I}_{0.04-0.21}[Mg_{0.80}Fe^{II-III}_{0.17}Al_{0.03}]\ [Si_{1.0}Al_{0.33}]\ O_{3.33}(OH)_{0.64}F_{0.03}, \tag{9}$$

or, with traditional normalization,

$$Ca_{0.13}M^{I}_{0.12-63}[Mg_{2.40}Fe^{II-III}_{0.51}Al_{0.09}]\ [Si_{3.00}Al_{0.99}]\ O_{10}(OH)_{1.92}F_{0.09}. \tag{9a}$$

As for phlogopite, however, these formulae are not compatible with the surface composition revealed by the X.p.s. analyses, the discrepancies being qualitatively similar though quantitatively less marked. Consequently we attempt a rationalization of the surface composition along similar lines. The small increase in the Si/Al X.p.d. range over that expected for complete isomorphous substitution indicates that only about 14% of the total Al content can occupy octahedral sites, so that x now becomes 1.30. Assuming that the iron content is the same as in the bulk, and still neglecting interlayer hydration, this leads to possible formulae (for the surfaces with the highest Al content) in the range

$$M^{I(\text{or equiv.})}_{0.40-0.23}[(Mg+Fe^{II})_{0.86-1.03}Fe^{III}_{0-0.17}Al_{0.08}]\ [Si_{1.0}Al_{0.48}]\ O_{3.70}(OH)_{0.71}F_{0.03} \tag{10}$$

(in which $Fe^{II}+Fe^{III} = 0.17$, the Fe^{II}/Fe^{III} ratio not being known *a priori*, and the octahedral M^{II} and M^{III} contents are inversely linked.) Although most vermiculites appear to contain predominantly Fe^{III} (Deer *et al.* 1962), the assumption of a high Fe^{III} content here would imply an improbably low layer charge, in view of the Pb-content detected in the fully-exchanged vermiculite. Whatever this ratio, however, we have, as with phlogopite, insufficient cations to fill all the octahedral sites, and the solutions to this enigma discussed in detail for that mineral apply equally here, although the anomaly is less marked.

The combination of X.p.d. and X.p.s. analysis, however, also gives us considerable insight into the interlayer composition of this mineral. We note first that the total detected interlayer ion (K, Ca) lost during exchange was considerably less than that gained (Pb): in the light of

our findings for both muscovite and lepidolite, however, this is hardly unexpected, and the total cation exchange capacity indicated by the Pb^{II} uptake matches the maximum suggested by the hypothetical formula (10) reasonably closely. The X.p.s. angular variation patterns however reveal further detail. Not only do the Si/K and Si/Ca plots (figure 7) show clear trends underlying the X.p.d. as the take-off angle increases, indicating that the cleavage plane itself is Ca-rich and K-deficient with respect to the immediately underlying layers, but also the diffraction patterns themselves are quite distinct. It follows that K and Ca cannot occupy equivalent sites in this natural vermiculite. After ion-exchange, however, the Si/Pb pattern matches that for Si/Ca quite closely, though with the changed concentration gradient the similarities are perhaps more qualitative than quantitative (see figure 8). One further change occurring in the X.p.s. as a consequence of ion-exchange is significant: the total oxygen content is increased very substantially (table 1), suggesting that the new Pb^{II} interlayer ion is fully hydrated. The parallel X.p.d. behaviour between Pb and Ca may then be taken to indicate that originally the calcium was hydrated but the potassium anhydrous: the immediate environment of the two ions, like their X.p.d. patterns, would then be quite different (coordination number 6 for Ca and Pb, but 12 for K). In confirmation of this, there are marked similarities between the X.p.d. pattern for Si/K in vermiculite and in lepidolite (figure 5), where the interlayer ion is believed not to be hydrated. Moreover, the calcium in a Ca-exchanged vermiculite has previously been found to be hydrated (d_{002} = 15.07 Å) in X-ray studies by Barshad (1948), whereas the potassium in the corresponding K-exchanged vermiculite had no hydration shell (d_{002} = 10.42 Å). The very variable intensity of the diffraction patterns for Ca (compare the three types of symbol in figure 7) probably reflects variations in the regularity of the hydration: the interlayer water may not always form well-ordered structures. The total oxygen contents before and after exchange as revealed by X.p.s. are in acceptable, if not quite quantitative, agreement with these suggestions (natural vermiculite; predicted 4.67 per Si, found 4.13: Pb-exchanged; predicted 5.61, found 5.6).† The principal conclusion is further reinforced by the X-ray diffractometer results: the expansion of the layer spacing on Pb-exchange is characteristic of the introduction of a hydrated interlayer typical of the ideal vermiculite, while the small 15.4 Å fraction revealed in the natural vermiculite may plausibly be attributed to hydrated calcium. The high calcium content at the cleavage may readily be explained by a tendency of the mineral to split along the hydrated interlayers where the silicate sheets are already more widely spaced than elsewhere.

It is interesting to note that these hydrated interlayers remain stable even in u.h.v. as long as the sample is not heated: one specimen, however, which was heated *in vacuo* to *ca.* 100 °C, exfoliated with considerable gas evolution. Hydrated lead ions are normally unstable *in vacuo*, as exemplified by the high decomposition pressure (*ca.* 9×10^{-3} Torr at 294 K) of, and known ease of water loss from, plumbous acetate trihydrate at room temperature. It is not, however, possible to ascertain whether the hydrated ions retained in the interlamellar regions of the vermiculite are stabilized kinetically or thermodynamically.

Finally, we compare the X.p.d. patterns for the vermiculite with those from lepidolite, the experimental axes of rotation having been almost identical (table 2) for these minerals. A rather close qualitative correspondence is apparent between the pairs of Si/K and Si/O diffraction patterns – reflecting the similar relative locations of Si, K and O in these minerals –

† These predictions assume that each Ca^{2+} or Pb^{2+} ion is accompanied by six water molecules, presumably in more or less octahedral coordination.

and also between Si/Mg in vermiculite and Si/Al in the lepidolite. This observation is particularly significant when it is recalled that the patterns for Si/Mg in phlogopite *failed* to match those for Si/Al in muscovite: it would thus appear that the large (*ca.* 30%) deficiency in the detected octahedral ion content near the exposed phlogopite surfaces is accompanied by a much more significant change in the local environment than occurs in the vermiculite, where the deficiency is much smaller ($\leqslant 12\%$). Note also that the clear parallels both between the natural and Pb-exchanged vermiculites and between the vermiculite and lepidolite X.p.d. patterns occur despite substantial variations in the interlayer spacing. The X.p.d. patterns would thus seem more sensitive to short-range than to long-range structural factors, although the very clear differentiation between the X.p.d. for the interlayer lead (if this element is indeed octahedrally coordinated) and octahedral structural magnesium would suggest that the structure beyond the immediate coordination sphere may be far from unimportant.

5. Concluding remarks

Studies of isomorphous substitution in complex monocrystalline solids can clearly be greatly assisted by the exploitation of angle-resolved X.p.s., as demonstrated in detail above. The new information obtained, quite apart from a comprehensive and essentially quantitative elemental analysis, concerns the relative locations of the different elements present. Examples have been described in which the phenomenon of X-ray photoelectron diffraction is used to identify the equivalence, near-equivalence, and non-equivalence of pairs of sites within the same crystal, and even (with some assistance from traditional X-ray crystallography to establish the sample alignment) to identify site similarities between different elements in discrete but structurally related crystals. Moreover, as a structural technique X.p.d. possesses two specific valuable characteristics. Provided only that adequate signal/noise ratios can be maintained, the technique can directly yield structural information relating to elements present in low concentration, in the present work down to 0.7% by weight (Na in muscovite). Such low concentrations are not an appreciable hindrance because the data are collected atom by atom and not, as with established X-ray methods, from the solid as a whole. Although the new techniques known as e.X.a.f.s. and ex.e.l.f.s. (see § 1) share this feature with X.p.d. – and yield closely related information – they require (unlike X.p.d.) considerable computation before any useful result is obtained. Unlike these techniques, however, X.p.d. cannot yet yield quantitative (numerical) data relating to nearest-neighbour separations or a partial radial distribution function. The second important feature is that an ordered array of the substitutional element is neither required, nor, indeed, helpful. It is sufficient simply that the sites be essentially equivalent; they may be occupied at random. In this again X.p.d. differs from X-ray crystallography, and from the established techniques of surface crystallography such as low energy electron diffraction. L.e.e.d. studies could indeed well complement X.p.d. in some instances, but the surface cleanliness requirements are far more stringent, and the information obtained would relate largely to the outermost atomic layer rather than to the whole near-surface region sampled in X.p.d.

The principal conclusions of the geochemical aspect of this work may be briefly summarized as follows. The accepted patterns of isomorphous substitution in muscovite and lepidolite, first obtained many years ago, largely from bulk chemical analyses and X-ray studies (Mauguin 1928; Pauling 1930), are entirely vindicated by the new X.p.d. data which, taken with the

concordant surface and bulk analyses, show conclusively that these specimens are essentially uniform in composition, despite small variations in the interlayer ion composition. The substantial fraction of the hydroxyl content of lepidolite and phlogopite which we found to have been replaced by fluoride in our specimens appears to be essentially randomly distributed, regions of facile cleavage not being associated with either unusually high or low concentrations of fluoride. This conclusion is compatible with recent theoretical studies. The composition of both the phlogopite and the vermiculite near regions of easy cleavage is, however, anomalous. Both minerals are nominally trioctahedral, with predominantly magnesium occupation of the octahedral sites, but in the cleavage region the total detected octahedral ion content is significantly deficient over the full X.p.s. sampling depth, while the aluminium content (relative to silicon) – and shown by the X.p.d. patterns to be almost entirely tetrahedrally coordinated – is considerably above that found in the bulk minerals. The structural changes which these local compositional anomalies imply would give rise to unusually high strains in the structure as a whole, and presumably are responsible for the propensity for cleavage of these specimens in such regions. However, whatever explanation is preferred, the reality of the compositional anomalies is clearly established, and our results, showing such effects in two out of the four more-or-less randomly selected specimens, suggest that such phenomena may be rather widespread, especially in those minerals where essentially full magnesium occupancy of the octahedral sites is normally assumed. The presence of both hydrated (Ca) and anhydrous (K) interlayer ions in natural (Transvaal) vermiculite, and the exchange of the latter for hydrated species (Pb) stable in u.h.v. are demonstrated, as is the preferential cleavage of this mineral in the hydrated regions.

We thank the S.R.C. for support, including the award of an Advanced Fellowship (S.E.), I.C.I. Ltd, for the gift of the vermiculite specimens, Dr E. S. Crawford and Dr D. A. Jefferson for supplying information before publication, and Dr D. A. Jefferson and Miss E. Raftery for experimental assistance.

References

Adams, J. M. & Evans, S. 1979 *Clays Clay Miner.* **27**, 137–139.
Adams, J. M., Evans, S., Reid, P. I., Thomas, J. M. & Walters, J. M. 1977 *Analyt. Chem.* **49**, 2001–8.
Adams, J. M., Evans, S. & Thomas, J. M. 1978*a* *J. chem. Soc., chem. Commun.*, 210–211.
Adams, J. M., Evans, S. & Thomas, J. M. 1978*b* *J. Am. chem. Soc.* **100**, 3260–2.
Baird, R. J., Fadley, C. S. & Wagner, L. F. 1977 *Phys. Rev.* B **15**, 666–671.
Barshad, I. 1948 *Am. Miner.* **33**, 655–678.
Bassi, I. W., Lytle, F. W. & Parravano, G. 1976 *J. Catal.* **42**, 139–147.
Bennett, H. & Reed, R. A. 1971 *Chemical methods of silicate analysis*. New York: Academic Press.
Crawford, E. S. 1978 Ph.D. Thesis, University College of Wales, Aberystwyth.
Deer, W. A., Howie, R. A. and Zussman, J. 1962 *Rock Forming Minerals*. Vol. 3. *Sheet Silicates*. London: Longman.
Dunham, P. C. & Wilkinson, F. C. F. 1978 *X-ray Spectrom.* **7**, 50–55.
Evans, S. 1977 In *Handbook of X-ray and UV photoelectron spectroscopy* (ed. D. Briggs), pp. 121–151. London: Heyden and Sons.
Evans, S. 1978 *Proc. R. Soc. Lond.* A **360**, 427–443.
Evans, S., Pritchard, R. G. & Thomas, J. M. 1977 *J. Phys.* C **10**, 2483–98.
Evans, S., Pritchard, R. G. & Thomas, J. M. 1978 *J. Electron Spectrosc. rel Phen.* **14**, 341–358.
Fadley, C. S. 1976 *Prog. Solid St. Chem.* **11**, 265–343.
Fadley, C. S. & Bergström, S. Å. L. 1971 In *Electron spectroscopy* (ed. D. A. Shirley), pp. 233–243. Amsterdam: North Holland.
Giese, R. F. 1978 *Clays Clay Miner.* **26**, 51–57.
Gruner, J. W. 1942 *Am. Miner.* **27**, 131–4.
Hill, J. M., Royce, D. G., Fadley, C. S., Wagner, L. F. & Grunthaner, F. J. 1976 *Chem. Phys. Lett.* **44**, 225–231.

Kincaid, B. M., Meixner, A. E. & Platzman, P. M. 1978 *Phys. Rev. Lett.* **40**, 1296–1299.
Leapman, R. D. & Cosslett, V. E. 1976 *J. Phys.* D **9**, L29–32.
Madey, T. E., Wagner, C. D. & Joshi, A. 1977 *J. Electron. Spectrosc. rel. Phen.* **10**, 359–388.
McConnell, D. 1950 *Am. Miner.* **35**, 166–172.
Mauguin, C. 1928 *Bull. Soc. fr. Minér. Cristallogr.* **51**, 285–332.
Pauling, L. 1930 *Proc. natn. Acad. Sci. U.S.A.* **16**, 123–129.
Pezerat, H. & Méring, J. 1967 *C. hebd. Séanc. Acad. Sci., Paris* D **265**, 529–532.
Powell, C. J. 1978 *Report of ASTM Committee E42 on Surface Analysis* (in preparation).
Siegbahn, K., Gelius, U., Siegbahn, H. & Olson, E. 1970 *Phys. Lett.* A **32**, 221–222.
Stern, E. A. 1974 *Phys. Rev.* B **10**, 3027–3037.
Thomas, J. (Jr.), Glass, H. D., White, W. A. & Trandel, R. M. 1977 *Clays Clay Miner.* **25**, 278–284.

PHILOSOPHICAL TRANSACTIONS OF THE ROYAL SOCIETY A MATHEMATICAL, PHYSICAL & ENGINEERING SCIENCES